

2.4 EXPERIMENTAL UPGRADED LAMP CONVECTION AND TOTAL LIGHTNING PROBABILITY AND “POTENTIAL” GUIDANCE FOR CONUS

Jerome P. Charba*
Frederick G. Samplatsky
Phillip E. Shafer
Judy E. Ghirardelli
National Weather Service, NOAA
Office of Science and Technology Integration
Meteorological Development Laboratory
Silver Spring, Maryland

Andrew J. Kochenash
KBRwyle Science, Technology & Engineering Group
Silver Spring, Maryland

1. INTRODUCTION

The history of the National Weather Service (NWS) Meteorological Development Laboratory (MDL) Localized Aviation MOS Program (LAMP) lightning and convection forecast products for the conterminous United States (CONUS) dates back to 2005 when Charba and Liang (2005) introduced LAMP experimental automated cloud-to-ground (CG) lightning (“thunderstorm”) probabilities. These lightning probabilities along with yes/no categorical forecasts, which are for 2-h valid periods in the 1-25 hour forecast range, were operationally implemented for 24 hourly cycles in 2008 (Charba and Samplatsky 2009). This product was targeted for use as guidance in the issuance of public, fire weather, and aviation forecast products. However, as convective storms sometimes occur without CG lightning, a new LAMP product called “convection” was developed specifically for aviation operations and planning (Charba et al. 2011), where the event consists of either radar reflectivity of ≥ 40 dBZ or CG strikes (or both). This new product involved upgrades to predictors used earlier for CG lightning, and the associated yes/no categorical forecasts were replaced with a multi-category convection “potential” product (<http://www.weather.gov/mdl/gfslamp/cnvtlg.php>). The upgrades were also incorporated in redevelopment of the CG lightning product; both products were operationally implemented in early 2014.

* Corresponding author address:
Dr. Jerome P. Charba, National Weather Service
1325 East West Highway, Room 10204
Silver Spring, MD 20910-3283
email: jerome.charba@noaa.gov

Subsequent feedback from users of these convection and lightning products has been generally favorable, but aviation community users of the convection product indicated a need for increased spatial and temporal resolution. In response, MDL has recently developed an upgraded LAMP convection product featuring increased resolution, which has been running experimentally since October 2016 (Charba et al. 2016; hereafter referenced as CS). In this upgrade radar reflectivity data from (now obsolete) Radar Coded Messages (RCM, OFCM 1991; Kitzmiller et al. 2002) were replaced with reflectivity products from the recently implemented Multi-Radar Multi-Sensor system (MRMS; Smith et al 2016; and Zhang, et al. 2016) and CG lightning flash data from the National Lightning Detection Network (<http://www.vaisala.com/en/products/thunderstormandlightningdetectionsystems/Pages/NLDN.aspx>) were replaced with recently implemented total lightning (TL) data [consists of both CG flashes and intra-cloud (IC) flashes], as provided by the Earth Networks Total Lightning Network (ENTLN, <https://www.earthnetworks.com/networks/lightning/>). Since user response to the upgraded convection guidance (<http://www.weather.gov/mdl/lamp/cnv1h.php>) has been quite positive, the same upgrades were subsequently incorporated into a new LAMP experimental total lightning product (<http://www.weather.gov/mdl/lamp/lgt1h.php>). These experimental products are expected to replace the currently operational convection and lightning products in July 2017.

CS contains a detailed description of the experimental convection model, but the article does not discuss model upgrades made quite recently, nor

does it discuss the experimental TL predictand. These topics are addressed here as well as operational versus experimental forecast performance comparisons for both the convection and lightning products.

2. LAMP MODEL UPGRADES

2.1 Upgraded Convection and Lightning Predictands

Distinguishing attributes of the LAMP operational and upgraded convection/lightning predictands are summarized in Table 1. Note that a principal upgrade to both predictands consists of doubling the temporal and spatial resolution, as the valid period was reduced from two hours to one hour and the valid area was “effectively” reduced from a 20-km square to a 10-km square¹. Supporting these predictand enhancements are upgrades to the underlying radar and lightning databases (Table 1). Benefits derived from replacing RCM reflectivity data with MRMS data result from superior numerical precision, temporal, and spatial resolution of the latter. Further, a supplemental automated quality control process developed at MDL is applied to the MRMS data, which enhances the value of this data input in these LAMP applications (Charba et al. 2017). For lightning, the data upgrade involved replacing CG lightning flashes from the NLDN with total lightning flashes (which includes IC flashes) from ENTLN. Charba et al. (2015) showed that IC flashes occur about five times as often as CG flashes in ENTLN data. Thus, these upgraded radar and lightning data likely improve the robustness of the LAMP convection and lightning predictands.

2.2 Upgraded Convection and Lightning Predictors

Upgraded predictor variables, which are matched with the convection and lightning predictands in the LAMP model, are summarized in Table 2 (see CS for additional details). It is important to note that relative to the LAMP model cycle time (denoted in the table as hh) the most recent MRMS and

TL observational predictors are valid at hh:15, and the most recent predictors from the High Resolution Rapid Refresh model [HRRR; Benjamin et al. (2016)] are from the (hh-1) hourly cycle to account for the ~1.5 hour HRRR model run time, and the LAMP forecast issuance in real time is by hh:45.

It is also important to note a special feature of the MRMS variables [namely, composite reflectivity (CREF) and vertically integrated liquid (VIL)]. Recall from section 2.1 that an MDL supplemental quality control (QC) process is applied to CREF, and when/where the QC determines a CREF value is not valid both it and the VIL value at the grid point are set to missing. In the subsequent MRMS predictor specification, these missing MRMS CREF and VIL observations are replaced with the most recent HRRR forecasts of simulated CREF and VIL. This replacement ensures production of non-missing LAMP convection and lightning forecasts over the entire CONUS domain, and for the western US, where network radar coverage is poor, it can improve the LAMP convection forecast patterns, as discussed in section 3.3.

3. PERFORMANCE OF CONVECTION AND LIGHTNING PROBABILITIES

3.1 Skill Score versus Forecast Projection

Since the upgraded predictor types are diverse (Table 2), ranging from fine-scale observations (obs) to fine-scale output from the HRRR and to large-scale MOS variables, it is useful to examine the sensitivity of LAMP probability skill to these three predictor types. Fig. 1 shows the Brier Skill Score [BSS; i.e., the Brier Score improvement on climatology², defined as the percentage improvement in $\frac{1}{2}$ the Brier Score (Brier 1950) for the convection probabilities over the corresponding score for convection relative frequency (Wilks 2006, pp. 284-285)] for the convection probabilities over the CONUS in the 1-16 hour LAMP forecast (projection) range. Note that when only MOS predictors are used the skill is relatively low and it decreases gradually with projection. Then, when HRRR predictors are added there is a substan-

¹The “upgraded” square gridbox is 20 km on a side, but since centers of these boxes are spaced 10 km apart, the size is 10 km in a practical sense. The rationale for maintaining the 20-km gridbox (where neighboring boxes overlap by 10 km) rather than changing to a 10-km box is to mitigate the undesirable reduction in event occurrence relative frequency that inherently accompanies the 50% valid period reduction.

² Climatology in this study consists of predictand relative frequency derived from the longest available historical sample for the particular convection or lightning predictand. For convection, the sample begins with January 2012; for lightning the sample begins with January 1994, and both samples end with September 2016. The relative frequencies are unique for each predictand grid box, valid period of the day, and day of the year.

tial increase in skill, and yet the MOS (only) and MOS+HRRR skill curves roughly parallel one another. Contrastingly, when obs predictors are added the resulting skill exhibits a striking upward jump at the 1-h projection³; afterward the skill drops sharply to 4 hours. This finding reveals a striking skill dominance of obs predictors for the very short projections.

Seasonal convection probability skill curves, using all three predictor types across the full 1-25 hour LAMP forecast range are shown in Fig. 2. These skill profiles exhibit three distinct features: (1) relatively high skill at short projections, which sharply decreases with projection (noted earlier) and reflects the heavy impact of obs predictors, (2) relatively moderate skill in the 4-16 hour range, which decreases gradually with time and reflects a major contribution from HRRR predictors, and (3) lower skill thereafter, where MOS predictors predominate. Note also that the shapes of the skill profiles are about the same across the three LAMP “seasons,” with the best skill over all projections during the cool season as convection occurs on relatively large space-time scales. Conversely, the weakest overall skill is for the summer season when convective scales are smallest.

Note that the convection skill curves in Fig. 2 are based on test regression equations where all three predictor types in Table 2 are screened for each LAMP forecast projection (HRRR predictors beyond the 17-h LAMP forecast projection consist of persistence of the 18-h HRRR forecast). However, since tests revealed the skill curves were essentially unchanged when the regression equations are derived with the three types of predictors segregated by LAMP forecast range as shown in Table 3, this segregation configuration was used to derive the final convection and lightning equations. Note also, that discarding the persisted HRRR predictors beyond 17 hours resulted in elimination of an often-seen distracting temporary pause of the LAMP forecast pattern with projection at 18 hours and beyond (not shown). Finally, note that HRRR and MOS predictors were based on the two most recent cycles rather than just the (single) most recent one. This too had little impact on the skill, though inspection of the forecasts for individual cases revealed that two cycles improved temporal continuity in the forecasts across projections and cycles.

³ At the 1-h projection [valid period = hh:00–(hh+1):00], a LAMP forecast is essentially a “nowcast” since it is not available to users until about hh:45.

3.2 Operational versus Experimental Probability Skill

Since the experimental convection and lightning guidance products were developed to replace the corresponding operational products, comparisons of forecast performance between them are relevant. BSS versus projection plots for the 2-h operational and 1-h experimental convection and lightning probabilities are shown in Fig. 3. Note that, while the operational and experimental BSS curves for either convection or lightning are plotted on a single chart, the BSS values can be compared only in a qualitative sense because the two predictands are unique. With this limitation in mind Fig. 3 shows that upgraded convection and lightning probabilities show higher skill (qualitatively) than the corresponding operational probabilities, especially for the short and middle projections. For these projections, the clear skill enhancement evidently reflects the contribution of the upgraded obs and HRRR predictors. Note that for projections in the 18-25 hour range the experimental probabilities show only a weak skill enhancement on the operational probabilities (MOS predictors are the predominant predictor input in each case).

3.3 Example Probability Maps

Peak probability skill at the 1-h LAMP projection for both convection and lightning was highlighted in the previous subsection. Figure 4 shows example experimental convection and lightning probability maps for a selected case at the 1-h forecast projection, which shows quite high spatial detail and sharpness in the probability patterns. Also shown in the figure are maps that serve as proxies for the verifying convection and lightning observations (see section 2.1 for definitions of the true convection and lightning predictand observations). Note the close match between the probability and the “observational” map patterns for both convection and lightning, which is expected for the 1-h LAMP forecasts since these are essentially “nowcasts,” as noted in section 3.1. The key point to be made here (for the 1-h projection) is the controlling influence of the MRMS and TL observational predictors in the respective convection and lightning probability patterns.

Another noteworthy feature in Fig. 4 is the striking reduction in area coverage in high probabilities from convection to lightning. This implies that key convection and lightning predictors are rather unique to each predictand. A predictor ranking analysis confirmed this finding (not shown), where the latest MRMS initial and advected CREF and VIL are key predictors for convection at the very short projec-

tions. Contrastingly, key corresponding predictors for lightning are the latest total lightning flash counts and their local time change. This predictor contrast results in substantial uniqueness in the convection and lightning probabilities because relatively high MRMS CREF values often occur with little or no lightning, especially during the cool season (the case in Fig. 4 happens to fall in the cool season). Thus, the convection and lightning forecasts can substantially complement one another, as seen for this case.

For LAMP projections in the 4-16 hour range we noted earlier that HRRR predictors have an important predictive role in the experimental convection model (Fig. 3; recall that HRRR predictors are not used in the corresponding operational models). Figure 5 contains a comparison of the operational and experimental convection probabilities for an 8-h projection for the same case as for Fig. 4. A striking feature in the experimental probabilities is the fine spatial detail and the high probability sharpness along a north-south line over the eastern US where there is a close match with high reflectivity features in the observed MRMS CREF map. This contrasts with a corresponding spatially-smearred pattern in the operational probabilities throughout the eastern US. Also, over the western US, the operational probabilities feature a localized peak along the WA-OR border, which is quasi-stationary across neighboring forecast projections (not shown). The experimental probability pattern is much more realistic there, with a uniform north-south alignment along the coastal mountain range, which shows consistency across forecast projections (also not shown). This pattern improvement stems from the MDL supplemental quality control of the MRMS observations, which results in extensive rejection of MRMS CREF observations in the area and their ensuing replacement with more-spatially-uniform HRRR 1-2 h CREF forecasts (Charba et al. 2017).

Turning to corresponding lightning forecasts (and observations) for this same case (Fig. 6), we see similar features over the eastern US, where the main distinction from convection is that both the operational and experimental probabilities are lower. Still, the experimental probabilities there show a close pattern match with the TL flash count map. Over the western US both the operational and experimental probabilities are near zero and essentially no TL flashes are found there. So, as found for the 1-h projection in this case, the convection and lightning probabilities complement one another, which may have guidance value for users.

4. “POTENTIAL” AND ITS PERFORMANCE

4.1 Specifying “Potential” from Probability

In the example case discussed in section 3, we saw that the magnitudes of convection and lightning probabilities can diminish substantially with increasing projection, and they can also exhibit substantial geographical variation for a given projection. Temporal and geographical variability of the probabilities result from inherent variations in convection and lightning predictability, which can make using the probabilities challenging. The conventional “remedy” for this problem is to convert the probabilities into “yes”-“no” categorical forecasts by deriving and then applying threshold probabilities.

CS extended the thresholding-categorization scheme by deriving and applying three probability thresholds to form three categories of predictand event “threat” (“risk”). A given probability threshold is derived from the developmental historical sample of probabilities by maximizing the threat score [same as the critical success index, Shaefer (1990)] with bias constrained to the narrow ranges shown in Table 4. Thus, a key feature of the probability thresholds and threat categories is that the bias range for a given potential threshold is known. For example, “low” threshold probability and “low” and above potential results in an over-forecasting bias (2.70 – 2.83; perfect bias = 1.0), medium and above potential yields a near perfect bias (bias just slightly above 1.0), and high potential strongly under-forecasts the predictand event (bias in the 0.38 – 0.43 range). So, an inherent attribute of potential is known, fixed bias, which is independent of LAMP forecast projection, time of the day, or geographical location. In this sense, LAMP convection or lightning potential has an advantage over LAMP probability, as the latter is often closely associated with forecast projection, time of the day, and geographical location.

It is worthy to note the LAMP convection and lightning probability models are highly stratified [i.e., by LAMP cycle, geographical region, and season (CS)]. Since the probability thresholds associated with potential are similarly stratified, the bias associated with potential is highly localized geographically, as well as by time of the day, and season.

Example maps that depict the conversion from convection probability to potential are shown in Fig. 7. As expected, the potential pattern is aligned with the probability pattern, which implies that increased spatial detail in the upgraded probabilities also appears in potential. Note also that the areal

coverage of low and above potential is far greater than that for high potential, which reflects the bias values in Table 4. Finally, close comparison of these maps reveals locations where a given potential level is associated with different probabilities than for another location. For example, medium potential along coastal Oregon and Washington is associated with probabilities of 25% or less, whereas medium over southern Alabama and western Florida is associated with probabilities well above 25%. Since the bias associated with medium and above potential (just above 1.0) is the same for both locations, potential should aid interpretation of the probabilities. Further, the bias standardization aspect of potential should be even more evident (and have even greater impact) when interpreting probabilities for short versus long projections, since probability differences at these contrasting ranges can be quite large.

4.2 Threat Score for Convection and Lightning Potential

A commonly used measure of performance for categorical forecasts is the threat score. Plots of threat score (for medium and above potential) versus forecast projection for the full CONUS domain are shown for both convection and lightning in Fig. 8, where each chart shows comparative scores for the 2-h operational and 1-h upgraded predictand. Note that for both convection and lightning these threat curves bear a close similarity to the corresponding skill curves in Fig. 3, which supports the robustness of both. Another consistent feature is the upgraded potential generally scores better than the operational potential, though for convection the two curves are almost coincident beyond the 17-h projection.

Also shown in an inset in each of the threat score charts in Fig. 8 is the average bias over the CONUS. Note that for both the upgraded convection and lightning potential, the average bias is very close to the medium and above bias “constraints” listed in Table 4. This demonstrates that the bias constraints used to derive the probability thresholds (using the dependent sample) are well reflected in the independent sample at hand.

5. CURRENT STATUS AND IMPLEMENTATION PLAN

The upgraded convection product has been running for all 24 cycles in experimental mode since June 2016; the upgraded lightning product has been running similarly since August 2016. Real time forecast maps for convection and lightning are available at http://www.weather.gov/mdl/lamp_experimental.

The convection product was evaluated by the National Centers for Environmental Prediction Aviation Weather Center (AWC) National Aviation Meteorologists located at the Federal Aviation Administration Command Center in Warrenton, VA and during the AWC 2016 Summer Experiment. The response to the convection products from both AWC groups was positive. Since the lightning products did not commence until late in the 2016 convective season, to date we have gotten little feedback from potential field users of this product.

A preliminary implementation date for the upgraded convection and lightning products had been tentatively set for April 2017, but unexpected delays in preparing the extensive implementation codes has resulted in a three month slippage to July 2017. With the implementation, the 1-h upgraded convection and lightning products will replace the corresponding 2-h products currently in operations.

6. SUMMARY

This article updates upgraded LAMP convection and lightning probability and potential guidance forecasts based on an earlier article (CS). The upgraded convection and lightning predictands have twice the spatial and temporal resolution than for currently operational convection and lightning products. The product upgrades and improved resolution result from the inclusion of recently-implemented MRMS and total lightning observations and HRRR model output. The study shows the upgraded convection and lightning probabilities have increased fine-scale detail and improved skill.

A product called “potential,” which is derived from the probabilities, is discussed to show how it can aid usage of the probabilities. The upgraded convection and lightning potential products also showed higher spatial detail and scored better than for the operational counterparts. The upgraded convection and lightning products are expected to replace the currently operational products by mid-2017.

7. ACKNOWLEDGEMENTS

Archived MRMS data and HRRR model output were provided by NOAA’s National Severe Storms Laboratory and the NOAA/Earth Systems Research Laboratory/Global Systems Division, respectively. Archived total lightning data were furnished by Earth Networks, Inc.

8. REFERENCES

- Benjamin, S. L., and Coauthors, 2016: A North American hourly assimilation and model forecast cycle: The Rapid Refresh. *Mon. Wea. Rev.*, **144**, 1669-1694.
- Brier, G. W., 1950: Verification of forecasts expressed in terms of probability. *Mon. Wea. Rev.*, **78**, 1-3.
- Charba, J. P., and F. Liang, 2005: Quality control of gridded national radar reflectivity data. Preprints, *21st Conference on Weather Analysis and Forecasting*, Washington, D.C., Amer. Meteor. Soc., **6A5**.
- _____, and F. G. Samplatsky, 2009: Operational 2-h thunderstorm guidance forecasts to 24 hours on a 20-km grid. Preprints, *23rd Conference on Weather Analysis and Forecasting/19th Conference on Numerical Weather Prediction*, Omaha, NE, **17B2**.
- _____, F. G. Samplatsky, and P. E. Shafer, 2011: Experimental LAMP 2-h convection guidance on a 20-km grid. Preprints, *24th Conference on Weather Analysis and Forecasting/20th Conference on Numerical Weather Prediction*, Seattle, WA, Amer. Meteor. Soc., **J19.3**.
- _____, F. G. Samplatsky, J. E. Ghirardelli, A. J. Kochenash, and P. D. Bothwell, 2015: Statistical properties of ENI IC/CG flashes relative to NLDN CG flashes over the CONUS. Preprints, *Seventh Conference on the Meteorological Applications of Lightning Data*, Phoenix, AZ, Amer. Meteor. Soc., **1.2**.
- _____, F. G. Samplatsky, and P. E. Shafer, J. E. Ghirardelli, and A. J. Kochenash, 2016: LAMP convection probability and "potential" guidance: An experimental hi-res upgrade. Preprints, *23rd Conference on Probability and Statistics in the Atmospheric Sciences*, New Orleans, LA, Amer. Meteor. Soc., **1.3**.
- _____, F. G. Samplatsky, and A. J. Kochenash, 2017: Supplemental automated quality control of MRMS reflectivity products for LAMP convection and lightning forecast guidance applications. Preprints, *28th Conference on Weather Analysis and Forecasting/24th Conference on Numerical Weather Prediction*, Seattle, WA, Amer. Meteor. Soc., **J6.1**.
- Kitzmler, D. H., F. G. Samplatsky, and D. L. Keller, 2002: Production of a national radar reflectivity mosaic and automated radar observations from WSR-88D radar coded messages. NOAA Tech. Memo. NWS MDL 83, National Oceanic and Atmospheric Administration, U.S. Department of Commerce, 23 pp.
- OFCM, 1991: Doppler radar meteorological observations: Part C, WSR-88D products and algorithms. Federal Meteorological Handbook 11, FMC-H11C-1991, Office of the Federal Coordinator for Meteorological Services and Supporting Research, Silver Spring, MD, 210 pp.
- Schaefer, T. J., 1990: The critical success index as an indicator of warning skill. *Wea. Forecasting*, **5**, 570-575.
- Smith, T. M., V. Lakshamanan, G. J. Stumpf, K. L. Ortega, K. Hondl, K. Cooper, K. M. Calhoun, D. M. Kingsfield, K. L. Manross, R. Toomey, and J. Brogden, 2016: Multi-Radar Multi-Sensor (MRMS) Severe Weather and Aviation Products. *Bull. Amer. Meteor. Soc.*, **97**, 1617-1630.
- Wilks, D. S., 2006: *Statistical Methods in the Atmospheric Sciences*. 2nd ed. Academic Press, 627 pp.
- Zhang, J., and Coauthors, 2016: Multi-radar multi-sensor (MRMS) quantitative precipitation estimation: Initial operating capabilities. *Bull. Amer. Meteor. Soc.*, **97**, 621-637.

Table 1. Aspects of LAMP operational and experimental convection and lightning predictands. Abbreviations: RCM = Radar Coded Messages; MRMS = Multi-Radar Multi-Sensor system; NLDN = National Lightning Detection Network; CG = cloud-to-ground lightning flash; ENTLN = Earth Networks Total Lightning Network; TL = CG + intra-cloud lightning (IC) flashes.

Predictand	Operational	Experimental
valid period	2 h	1 h
valid area	20-km gridbox	10-km gridbox
radar database	RCM	MRMS
lightning database	NLDN CG	ENTLN TL

Table 2. Observational (obs; a), High Resolution Rapid Refresh (HRRR; b), and Model Output Statistics (MOS; c) predictor variables for LAMP convection and lightning predictands. In (a) hh denotes the LAMP model cycle time, where hh = 00, 01, ... , 23. Each obs predictor is specified as “initial” and “advected” (see Charba et al. 2016). Abbreviation in (a): max = maximum value in a 10-km gridbox.

(a) Obs

Multi-Radar Multi-Sensor system (MRMS) max composite reflectivity (CREF) valid at hh:15
 MRMS max CREF valid at (hh-1):45
 MRMS max CREF valid at hh:15 – MRMS max CREF valid at (hh-1):45
 MRMS max vertically-integrated liquid (VIL) valid at hh:15
 60 min total lightning flash (TL) count ending at hh:15
 30 min TL count ending at hh:15
 30 min TL count ending at hh:15 – 30 min TL count ending at (hh-1):45

(b) HRRR

CREF
 VIL
 1-h total precipitation amount
 precipitable water
 surface moisture divergence
 lifted index
 convective available potential energy
 lightning threat

(c) MOS

GFS-based (and NAM-based) predictand probability
 GFS-based predictand probability x NAM-based predictand probability
 GFS-based (and NAM-based) predictand probability x predictand monthly relative frequency
 GFS-based (and NAM-based) predictand probability x gridded terrain elevation

Table 3. Predictor type versus LAMP forecast projection range (hours). ✓ symbol denotes that a predictor type was used for a given forecast range.

Predictor type	1 – 12	11 – 14	14 – 17	16 - 25
MRMS + total lightning observations *	✓			
HRRR forecasts	✓ **	✓ **	✓	
GFS/NAM MOS probability	✓	✓	✓ **	✓ **

* Initial + advected

** Two latest model cycles

Table 4. Basic aspects of the specification of potential from probability.

Threshold probability	Convection threat category	Bias range
low	low	2.70 – 2.83
medium	medium	1.03 – 1.13
high	high	0.38 – 0.43

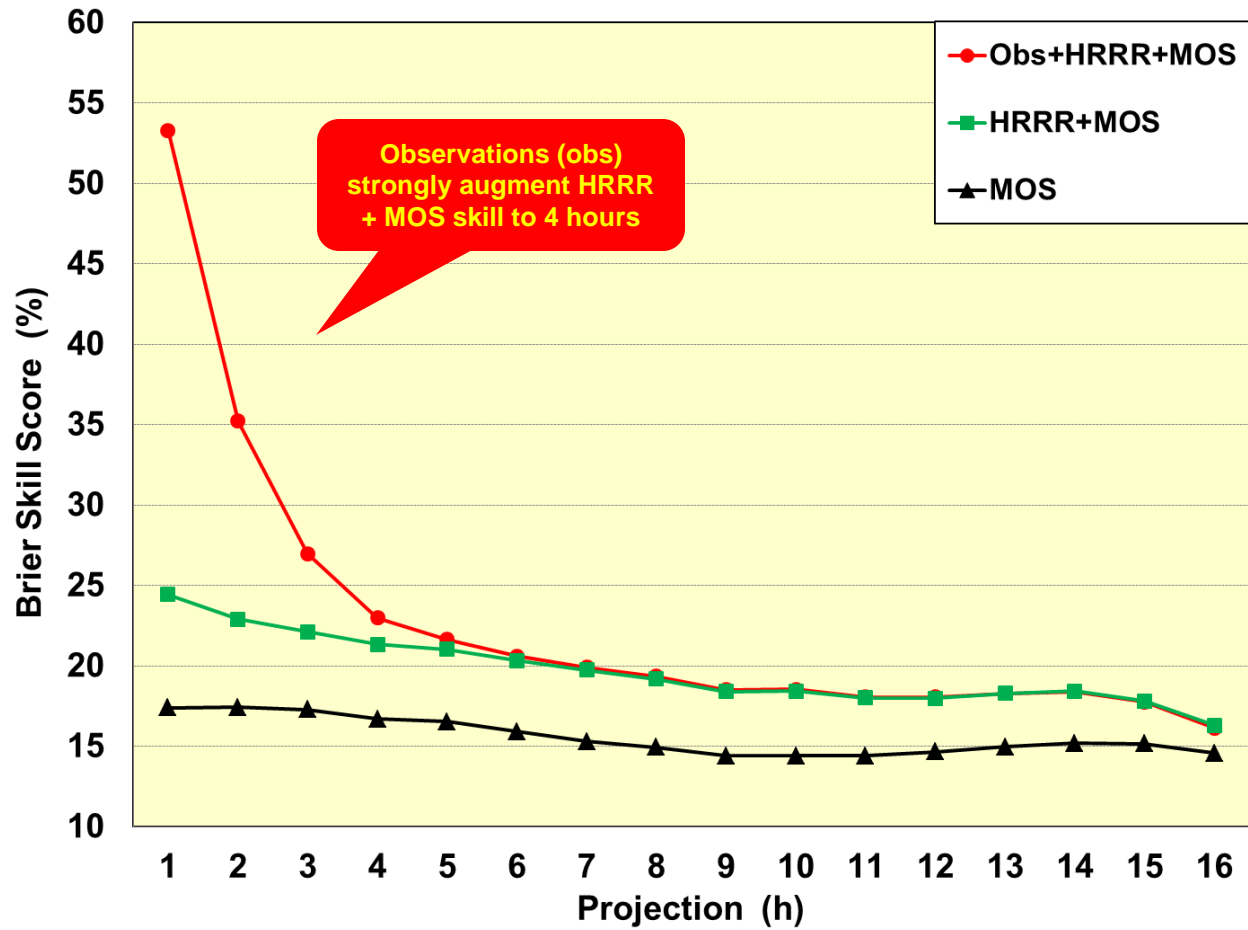


Figure 1. Brier Skill Score for LAMP convection probability versus forecast projection (limited to 16 hours) for the three types of predictors shown in Table 2. The test sample consists of the 1800 and 0600 UTC LAMP cycles combined for 216 days uniformly selected from 01 January 2012 – 31 May 2016.

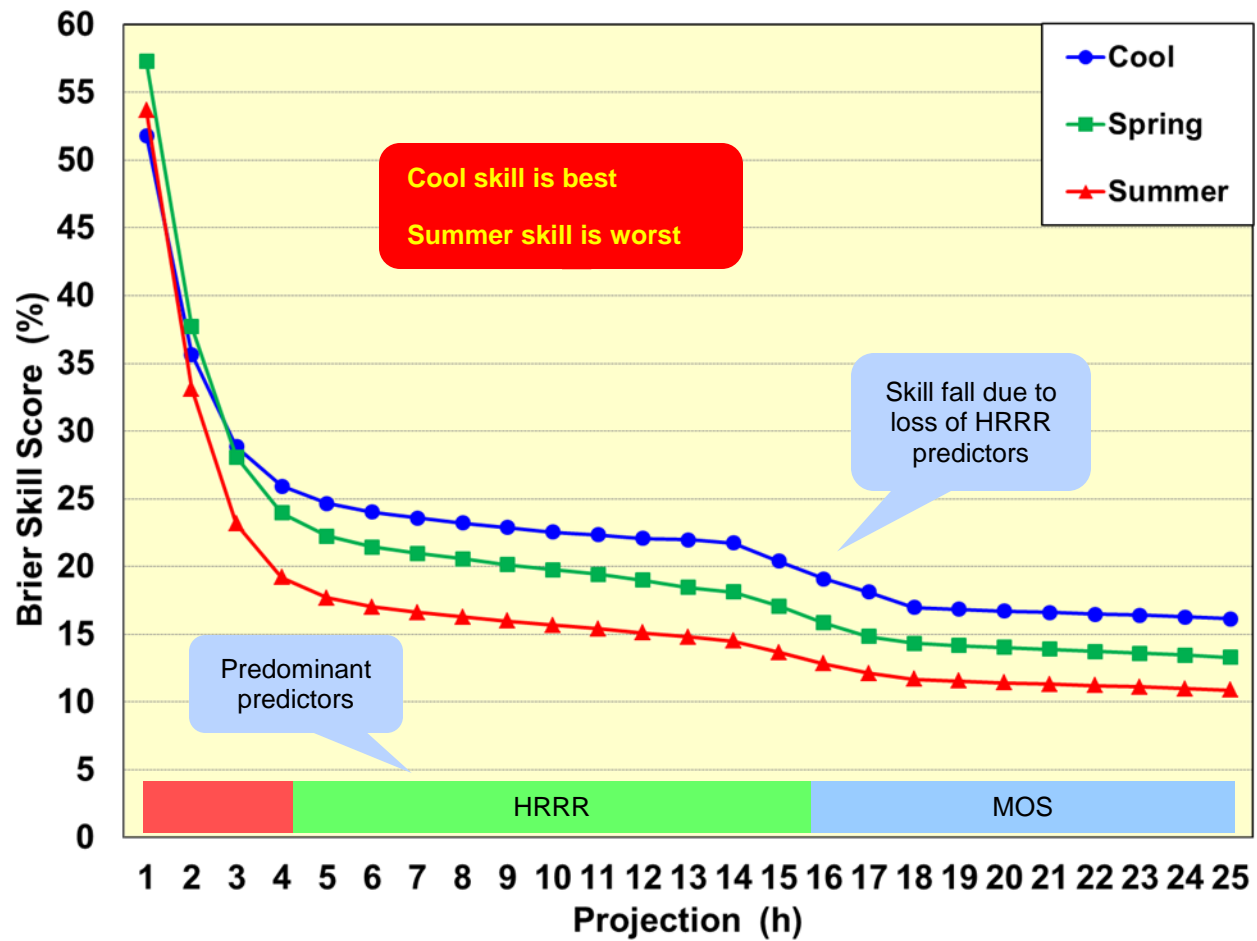


Figure 2. Brier Skill Score versus forecast projection (full 25-h range) for convection probabilities for three LAMP seasons (cool = 16 October – 15 March; spring = 16 March – 30 June; summer = 1 July – 15 October). The skill scores (dependent) are based on all 24 LAMP cycles combined and all days from 01 January 2012 – 31 May 2016. The predominant predictor types shown are defined in Table 2.

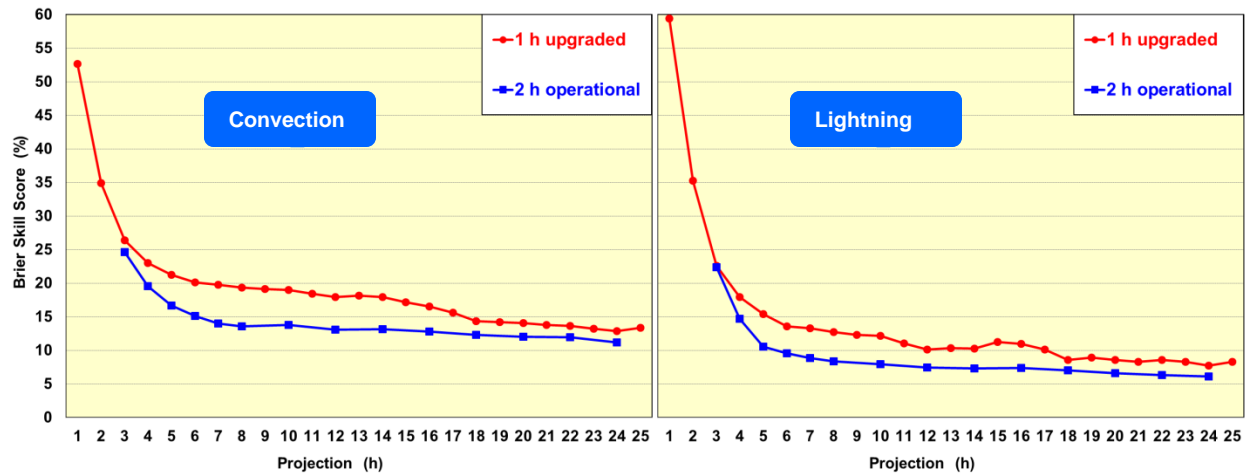


Figure 3. Brier Skill Score versus forecast projection for operational (2 valid period) and upgraded (1-h valid period) LAMP convection (left) and lightning (right) probabilities averaged over the full CONUS domain. The verifying observation used for the operational and upgraded predictand (for both convection and lightning) in each case was consistent with predictand definition. The test sample consists of the 1800 and 0600 UTC cycles combined for 246 evenly spaced days from 06 May 2014 – 31 May 2016.

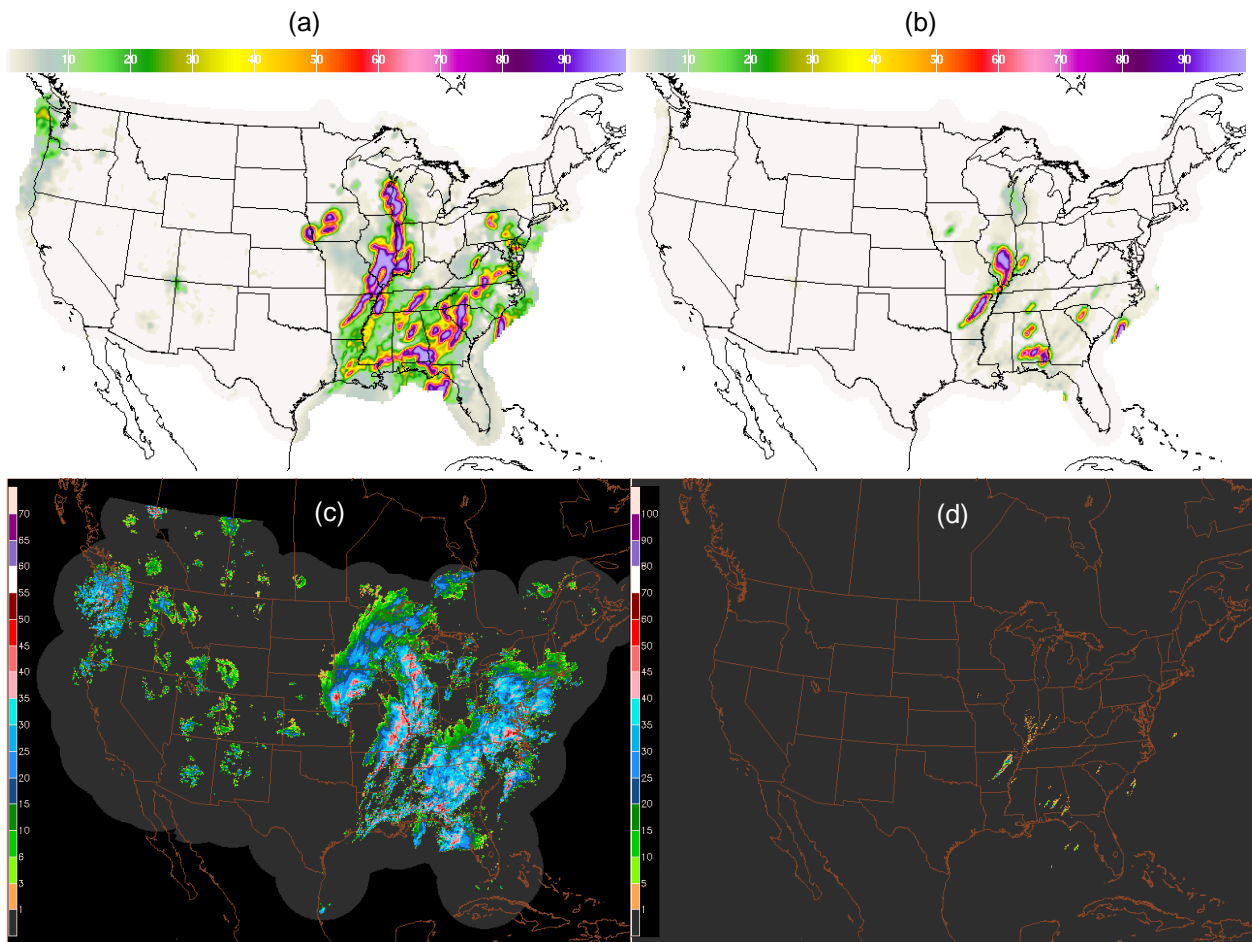


Figure 4. (a) Experimental convection probability (%) and (b) experimental lightning probability (%) valid 1800 - 1900 UTC 23 December 2015 (see text). (c) Contoured MRMS maximum composite reflectivity (dBZ) in 5-km grid boxes at 1830 UTC and (d) total lightning flash count in 5-km gridboxes during 1800 - 1900 UTC serve as proxies for the verifying convection and lightning predictand observations.

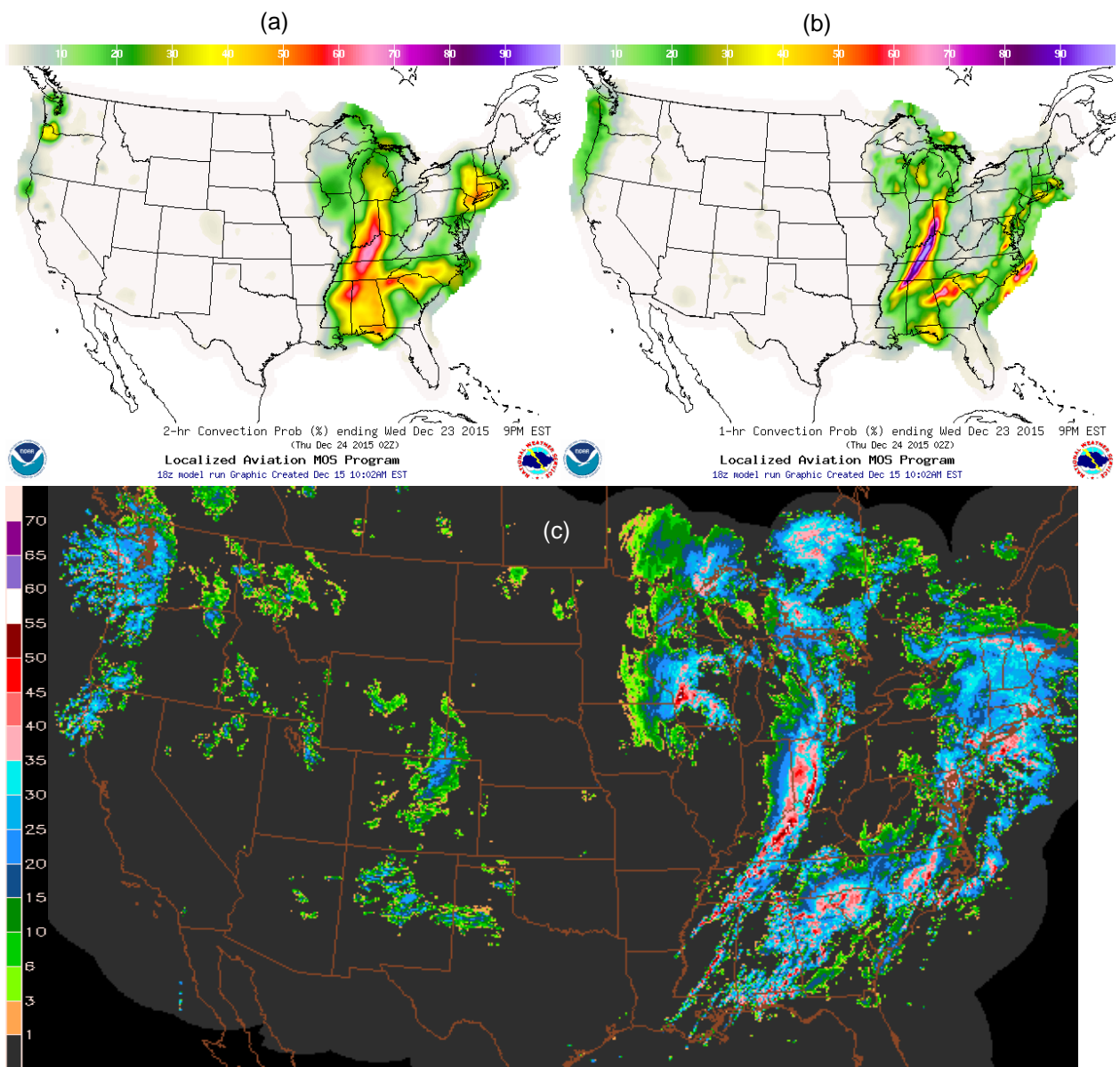


Figure 5. (a) Operational 8-h convection probability forecast (%) valid 0000-0200 UTC from the 1800 UTC LAMP cycle on 23 December 2015, (b) corresponding experimental convection probability (%) valid 0100-0200 UTC, and (c) maximum MRMS composite reflectivity (dBZ) in 5-km gridboxes valid at 0130 UTC. The latter map serves as a proxy for the verifying convection observations for both the operational and experimental probabilities.

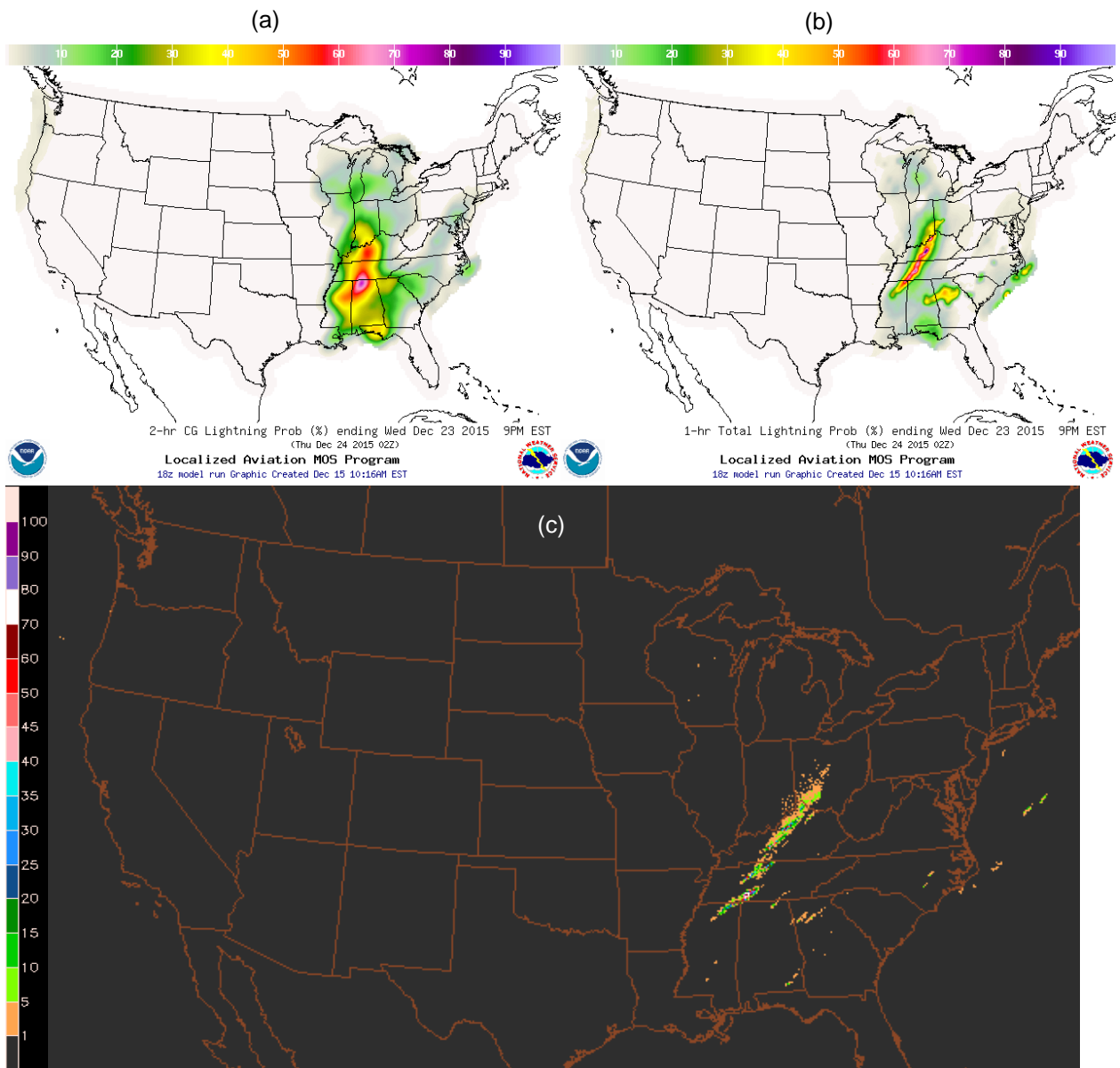


Figure 6. (a) Operational 8-h CG lightning probability forecast (%) valid 0000-0200 UTC from the 1800 UTC LAMP cycle on 23 December 2015, (b) corresponding experimental total lightning probability (%) valid 0100-0200 UTC, and (c) TL flash count in 5-km grid boxes during 0100-0200 UTC. The TL flash count map serves as a proxy for the verifying lightning observations for both the operational and experimental probabilities.

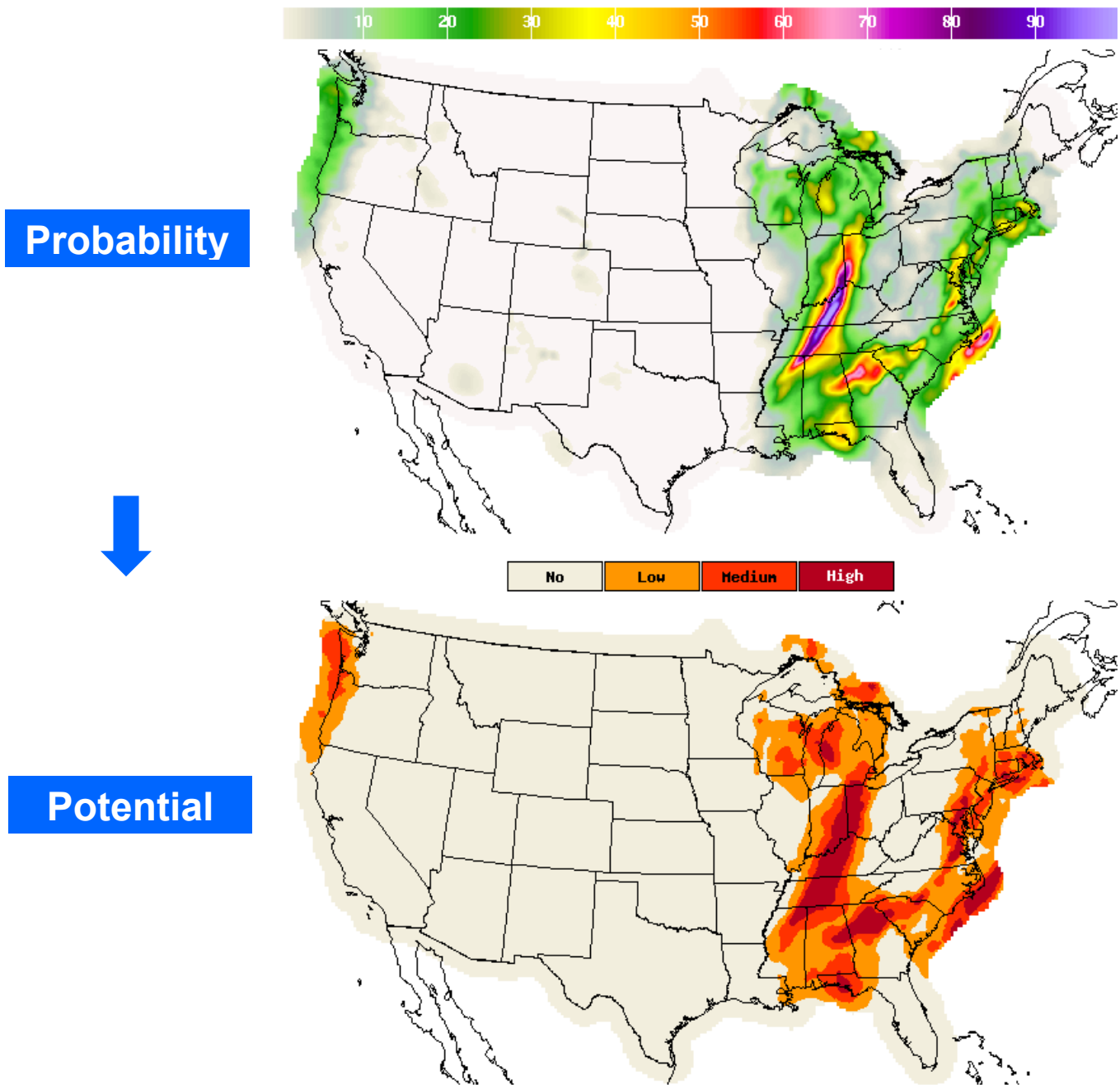


Figure 7. Example maps of convection probability and potential to illustrate the conversion from the former to the latter.

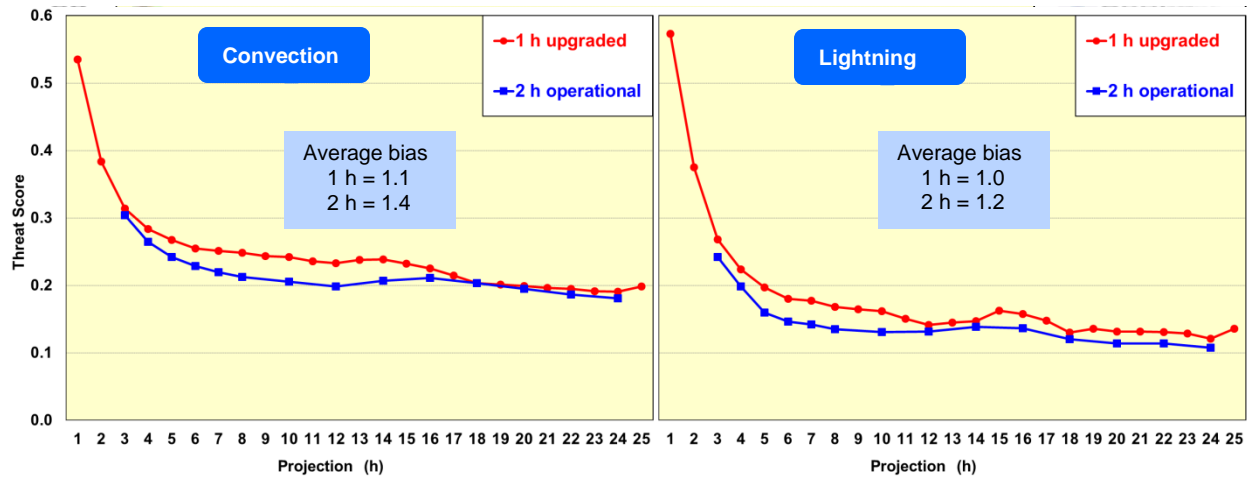


Figure 8. As in Fig. 3 except for threat score for medium and above potential. CONUS average bias scores are shown as an inset in each chart.